Fibronectin Type III Domain Based Monobody with High Avidity†

Jinzhu Duan,‡ Jinsong Wu,‡ C. Alexander Valencia, and Rihe Liu*

School of Pharmacy and Carolina Center for Genome Sciences, University of North Carolina at Chapel Hill, Chapel Hill, North Carolina 27599

Received June 19, 2007; Revised Manuscript Received August 13, 2007

ABSTRACT: Significant efforts have been made to improve the target-binding strength of numerous affinity molecules that are widely used in biomedical research and clinical applications. While many antibody-like fragments have been successfully optimized through affinity maturation, the process is time-consuming and restricted by the stability, solubility, and expression level of the protein sequences. To generate a fibronectin type III domain (FN3) based monobody that binds to the tumor-related biomarkers with exceptional high strength and stability, we developed a multivalent strategy by fusing an $\alpha_v\beta_3$-binding FN3 monobody with a short COMP pentamerization domain through a linker that facilitates appropriate display of multivalent FN3 domains. The fusion protein was highly expressed in the soluble fraction of *Escherichia coli* and efficiently self-assembled into a pentameric molecule that could be readily purified. Compared to the monomeric form, the pentameric monobody bound to $\alpha_v\beta_3$ integrin much more tightly with significantly slower off-rate, while still maintaining its excellent specificity toward $\alpha_v\beta_3$ when tested by using purified integrins and integrin-expressing cell lines. The multivalent strategy we describe here could be applied to engineer other FN3 monobodies to acquire significantly improved targeting-binding strengths.

Target-binding affinity molecules are of great importance in numerous biomedical applications. One of the major challenges in engineering an affinity molecule is to improve its target-binding strength and specificity. While most naturally occurring antibodies are large proteins that are difficult to express and engineer, the use of antibody fragments represents an interesting compromise. Various target-binding antibody fragments have been developed, including F_{ab} fragments, single-chain antibodies, isolated V_L [1] and V_H domains, and helix-stabilized antibody fragments. A different approach is to select small antibody mimics from combinatorial peptide libraries based on protein scaffolds related or not related to natural antibodies. Among numerous scaffolds that have been used to evolve affinity molecules, the tenth type III domain of human fibronectin (FN3) has several unique advantages. The structure of FN3 is best described as a β-sandwich similar to that of the V_H domain, with the CDR-like ligand binding sites formed by the three surface loops (*1*−*5*). Therefore, a scaffold-based monobody library can be generated by randomizing residues on surface loops and used in the selection of affinity molecules that target various biomarkers. FN3-based monobodies thus generated are ideal for large-scale expression in bacteria, presumably due to its small size (less than 100 residues), exceptional thermostability ($T_m \sim 90$ °C), and lack of disulfide bonds. In addition, FN3 monobodies are presumably less immunogenic due to the extreme abundance of FN3 on human cell surface receptors (*6*−*10*). Koide and co-workers reported the first use of FN3 as a scaffold for the single domain antibody mimics (*11*−*13*). Since then, FN3 monobodies that target ubiquitin, Src SH3 domain, streptavidin, TNF-α, $\alpha_v\beta_3$, and VEGF receptor have been reported by different groups (*11*, *14*−*20*).

Compared to full-size antibodies, unengineered monobodies bind to their targets less tightly, presumably due to their greatly reduced surface areas that are available for protein−protein interactions. Indeed, both the naturally occurring $\alpha_v\beta_3$-binding FN3 domain and the ubiquitin-binding FN3 monobody isolated from a phage-displayed library bind to their targets with micromolar affinities. Although the binding affinities can be further improved through extensive affinity maturation, the process is time-consuming and limited by the stability, solubility, and expression level of the optimized sequences.

One of the most effective approaches used in nature to achieve strong binding between an antigen and its antibody is through multivalent interactions. Naturally occurring IgM antibodies, for example, bind to antigens very tightly and efficiently, although the antigen-binding affinity of its monomeric form is relatively weak. This functional affinity or avidity of multiple antibody−antigen interactions when more than one interaction takes place between two molecules can be orders of magnitude higher than the intrinsic affinity of a single antibody−antigen interaction (*21*). It is expected

† This work was supported by a grant from the National Cancer Institute to the Carolina Center of Cancer Nanotechnology Excellence (Grant U54 CA119343).

* To whom correspondence should be addressed. Telephone: (919) 843-3635. Fax: (919) 968-0081. E-mail: rihe_liu@unc.edu.

‡ These authors contributed equally to the work.

[1] Abbreviations: CDRs, complementarity determining regions; COMP, cartilage oligomeric matrix protein; FN3, the tenth fibronectin type III domain; HBSS, Hank's buffered salt solution; HRP, horseradish peroxidase; Ig, immunoglobulin, IMAC, immobilized metal ion affinity chromatography; IPTG, isopropyl β-D-1-thiogalactopyranoside; T_m, melting temperature; V_H, variable domain of Ig heavy chain; V_L, variable domain of Ig light chain; VEGFR, vascular endothelial growth factor receptor.

10.1021/bi701215e CCC: $37.00
Published on Web 10/12/2007

that such multivalent interaction significantly increases the local concentration of the affinity unit, thus effectively providing a decreased overall off-rate. The net effect is that the stability of the target/affinity molecule complex is greatly increased. So far, the multivalent strategy has been successfully used to increase the target-binding strength of a number of homing short peptides and antibody fragments (*21*−*23*).

Integrin $\alpha_v\beta_3$ is a multifunctional glycoprotein formed by noncovalent association of a 125 000 α_v subunit and a 105 000 β_3 subunit. It plays a major role in several distinct processes, including angiogenesis, osteoclast-mediated bone resorption, pathological neovascularization, and tumor metastasis (*24*, *25*). Integrin $\alpha_v\beta_3$ has been shown to be overexpressed specifically on the surface of proliferating vascular endothelial cells and mediate their interactions with extracellular matrix, and thus play a key role in the angiogenic cascade (*24*, *25*). To develop affinity molecules that bind to the tumor-related biomarkers with exceptional high strength and stability, we report here the generation of an $\alpha_v\beta_3$-binding FN3 monobody that can be highly expressed and efficiently self-assembled into a pentameric form. The resulting pentameric monobody is very stable and specifically binds to $\alpha_v\beta_3$ with much higher strength than the monomeric form. This multivalent strategy might be used to systematically engineer other FN3 monobodies to acquire significantly improved target-binding strength.

EXPERIMENTAL PROCEDURES

Generation of the Expression Vectors. A synthetic gene that codes for $FN3^{\alpha v\beta 3}$-COMP was synthesized and confirmed by sequencing. The amino acid sequence of $FN3^{\alpha v\beta 3}$ is the same as that previously reported by Dewhurst and coworkers (*17*). The pentamerization domain used here is a modified version of the N-terminal fragment of mouse cartilage oligomeric matrix protein (COMP). This COMP domain has 55 amino acids and tends to form a five-stranded α-helical coiled-coil (*22*, *26*). The amino acid sequence of the COMP domain used in this work was GGDCCPQML-RELQETNAALQDVRELLRQQVKEITFLKNTVM-ECDACGMQ PARTPG, as reported by Mach and coworkers (*22*). It is worth mentioning that both Leu29 and Ala30 were substituted with Cys to facilitate the formation of interchain disulfide bonds near the N-terminus of the helix (*22*). The sequence of the linker between FN3 monobody and COMP domain is GGLNDIFEAQKIEWHEGKKGKG-PQPQPKPQPQPQPQPKPQP KPEPE, which includes a 13-residue helical region followed by a flexible hinge region. The coding sequence for $FN3^{\alpha v\beta 3}$-COMP was synthesized as a synthetic gene at Genscript (Piscataway, NJ). After confirmation by sequencing, the coding sequences were PCR amplified and cloned into a pET-28b expression vector (Novagen, Madison, WI) between *Nde I* and *BamH I* sites. The resulting expression vectors $pJDFN3^{\alpha v\beta 3}$ and $pJDFN3^{\alpha v\beta 3}$-COMP were confirmed by sequencing and used for overexpression of monomeric $FN3^{\alpha v\beta 3}$ and pentameric $FN3^{\alpha v\beta 3}$-COMP, respectively.

Overexpression of $\alpha_v\beta_3$-Binding FN3 Monobodies in Escherichia coli. Monomeric $FN3^{\alpha v\beta 3}$ and pentameric $FN3^{\alpha v\beta 3}$-COMP were overexpressed in *Escherichia coli* (*E. coli*) BL21(DE3). About 500 mL of LB medium in a 2 L baffle flask was inoculated with 5 mL of an overnight culture. IPTG was added at a final concentration of 0.5 mM to initiate protein expression, together with 50 μg/mL of free biotin if biotinylation of the overexpressed proteins was desired, when OD_{600} reached 0.7, followed by shaking for another 4 h at 30 °C. The cells were harvested by centrifugation at 4000 rpm for 15 min, and the pellets were stored at −80 °C until further use.

Purification of Overexpressed Monobodies and Separation of the Pentameric Form. The pellets were suspended in 50 mL of immobilized metal ion affinity chromatography (IMAC) binding buffer (20 mM Tris-HCl, pH 8.0, 0.5 M NaCl, and 10 mM imidazole), and cells were homogenized by ultrasonic treatment. The supernatant was collected by centrifugation at 12 000 rpm for 10 min and loaded into a Bio-Rad column with 7 mL of chelating Sepharose fast flow resin (GE, Piscataway, NJ) at room temperature. The column was washed with 10 column volumes of binding buffer, followed by 10 column volumes of wash buffer containing 60 mM imidazole. The His×6-tagged proteins were eluted with an appropriate volume of elution buffer containing 250 mM imidazole. The fractions containing the proteins of interest were pooled and dialyzed with Tris buffered saline (TBS) and stored at −20 °C until required.

Pentameric $FN3^{\alpha v\beta 3}$-COMP was further purified by gradient elution on an IMAC column. Briefly, 0.6 mg of proteins purified after the first IMAC column were reloaded into a column with 1 mL of chelating Sepharose fast flow resin in a binding buffer containing 50 mM imidazole. The bound proteins were then sequentially eluted using 10 column volumes of 150 mM imidazole, 5 column volumes of 180 mM imidazole, 5 column volumes of 200 mM imidazole, and 4 column volumes of 250 mM imidazole in the binding buffer, respectively. Protein concentrations were determined by the Bradford assay and confirmed by SDS-PAGE analysis and Coomassie brilliant blue staining. If free biotin was not added for enzymatic biotinylation during overexpression, the purified recombinant proteins were chemically biotinylated for comparison purposes using NHS-PEO_4-Biotin (Pierce, Rockford, IL) according to the manufacturer's instructions.

ELISA Analysis of $\alpha_v\beta_3$-Binding Properties. To investigate the binding of the biotinylated monomeric $FN3^{\alpha v\beta 3}$ and the pentameric $FN3^{\alpha v\beta 3}$-COMP with different human integrins by ELISA, purified $\alpha_1\beta_1$, $\alpha_5\beta_1$, $\alpha_v\beta_3$, or $\alpha_v\beta_5$ were incubated overnight in a high-binding EIA/RIA plate (Corning, Acton, MA) at a concentration of 5 μg/mL in a TBS buffer at 4 °C. The plate was washed 3 times with TBS buffer and blocked for 2 h at room temperature with a blocking buffer (0.5 mg/mL BSA in 0.1 M Na_2CO_3, pH 8.6). Biotinylated monobodies with different concentrations were then added in a binding buffer containing 1 × TBS, 0.1% Tween-20, and 2 mM $CaCl_2$. After the plates were washed 10 times, 0.1 μg/mL of neutravidin-HRP was added with the binding buffer. The plates were incubated for 1 h at room temperature and washed 10 times. Bound HRP was detected by adding 0.5 mg/mL of OPD substrate (Pierce) in a stable peroxide substrate buffer (Pierce). Color was developed for 10 min before reading the OD_{492} with a Bio-Rad 3350 microplate reader.

Dot Blotting Analysis of $\alpha_v\beta_3$-Binding Properties. The monomer or the pentamer was spotted at various concentrations (10 nM to 2 μM) onto nitrocellulose membranes using a Bio-Dot apparatus (Biorad, Hercules, CA). The protein

spots were air-dried for 30 min. The membranes were washed twice with TBST−$CaCl_2$ buffer (25 mM Tris, pH 8.0, 150 mM NaCl, 0.1% Tween-20, and 1 mM $CaCl_2$) and blocked with 3% BSA (w/v) in TBST−$CaCl_2$ for 1 h. After thorough washes, membranes were incubated for 1 h at room temperature with 5 μg/mL of $\alpha_V\beta_3$ in TBST−$CaCl_2$ containing 3% BSA. Membranes were washed and probed for 1 h at room temperature with an anti-$\alpha_V\beta_3$ antibody (Chemicon, Temecula, CA) at a final concentration of 2 μg/mL. For detection of signal, blots were washed and probed with anti-mouse Ig-HRP (Amersham, Piscataway, NJ) followed by development using an ECL plus system (Roche, Indianapolis, IN).

BIAcore Analysis. Purified human $\alpha_v\beta_3$, $\alpha_1\beta_1$, $\alpha_5\beta_1$, and $\alpha_v\beta_5$ integrins (Chemicon, Temecula, CA) were immobilized on research grade CM5 sensor chips using an amine coupling kit supplied by the manufacturer (BIAcore, Piscataway, NJ). Conjugation was performed in 10 mM sodium acetate (pH 4.5) at a concentration of 5 μg/mL of integrin with a surface density around 1000 resonance units (RU). The FN3$^{\alpha v\beta 3}$ or the FN3$^{\alpha v\beta 3}$-COMP with various concentrations (4 nM to 32 nM) were injected into the flow cell in an HBS−P buffer (10 mM HEPES pH 7.4, 150 mM NaCl, 0.005% surfactant P20) supplemented with 2 mM $CaCl_2$ at a flow rate of 20 or 40 μL/min. To measure the binding affinity using immobilized monobodies, neutravidin (Pierce) was first conjugated to a CM5 chip followed by immobilizing an appropriate amount of biotinylated monomer or pentamer at a surface density around 500 RU. Purified human integrins were then injected at different concentrations in the same buffer. The binding constants were calculated by fitting the BIAcore data to a 1:1 interaction model. Data were calculated using the BIAevaluation 3.0 software from BIAcore.

Protease Resistance. The protease digestion was performed by mixing 2 μg of the purified monomeric or pentameric monobody with 20 ng of thermolysin (Sigma, St. Louis, MO) in 30 μL of HBS buffer supplemented with or without 1 mM DTT. The reaction mixture was incubated for 15 min at 4, 25, 37, and 42 °C, respectively, followed by adding 15 μL of 4× SDS-PAGE buffer with or without reducing agent to terminate the digestion. A reaction mixture without the protease was used as a control. A 20 μL aliquot of each sample was then loaded to an SDS-PAGE gel for separation under nonreducing or reducing conditions. The proteins were stained using Coomassie brilliant blue.

Thermal Stability. CD spectra were recorded with an Aviv Model 202-01 spectropolarimeter at the UNC Macromolecular Interactions Facility. The analyses were performed in a 10 mM phosphate buffer at pH 7.5 using circular cuvettes with path lengths of 0.1 cm. Spectra were recorded from 190 to 260 nm at 0.2 nm intervals, a scan speed of 20 nm/min, a bandwidth of 2 nm, and an integration time of 1 s. Protein spectra were subtracted from the background. To determine T_m values, sample temperatures were increased gradually from 25 to 95 °C. Spectra were recorded at various temperatures following a 10 min equilibration time. An average of multiple measurements of the ellipticities at 215 nm with 70 μg/mL of the monomeric FN3$^{\alpha v\beta 3}$ or that at 209 nm with 40 μg/mL of the pentameric FN3$^{\alpha v\beta 3}$-COMP was used to plot the graph of ellipticity versus temperature.

Cell Culture. K562, K562-$\alpha_v\beta_3$, and K562-$\alpha_v\beta_5$ cells were a generous gift from Dr. S. Blystone at Upstate Medical University. The cells were maintained in Iscove's modified Dulbecco's medium (IMDM) (Invitrogen, La Jolla, CA) or RPMI 1640 supplemented with 10% FBS, 1% penicillin-streptomycin, 2 mM L-glutamine, and 500 μg/mL of G418 at 37 °C and 5% CO_2.

Detection of Cell-Binding of Monomeric FN3$^{\alpha v\beta 3}$ and Pentameric FN3$^{\alpha v\beta 3}$-COMP Using Confocal Microscopy. Approximately 200 μL of the biotinylated monomer or pentamer at various concentrations (10 to 100 nM for pentamer; 10 nM to 2 μM for monomer) were mixed with 5 μg/mL of streptavidin−Alexa Fluor 555 for 1 h at room temperature in HBSS−$CaCl_2$. The mixture was added to approximately 1×10^6 K562-$\alpha_v\beta_3$ or K562-$\alpha_v\beta_5$ cells and incubated for 1 h at room temperature. After binding, cells were washed twice with HBSS−$CaCl_2$ and mounted with Fluoromount-G onto fluorescent slides (Gold Seal, Portsmouth, NH) and examined using a Zeiss LSM5 Pascal confocal microscope.

RESULTS

Design of FN3$^{\alpha v\beta 3}$ Pentamer. To develop an FN3 based monobody that binds to tumor-related biomarkers with exceptional high strength and stability, we fused an $\alpha_v\beta_3$-binding monobody with the COMP assembly domain that can self-assemble into a five-stranded α-helical bundle with high stability (*26*−*28*). To make the system suitable for displaying five FN3 monobodies each with approximately 100 amino acids, we extended the linkage between FN3 and COMP domains. Such linkage consists of a 20 amino-acid relatively rigid helix (GGLNDIFEAQKIEWHEGKKGK) followed by a 25 amino-acid flexible nonstructural hinge region (GPQPQPKPQPQPQPQPKPQPKPEPE). We postulated that such extension would provide enough space to accommodate five monobodies on the core while still maintaining the right geometry of the pentameric structure. It appeared that the length rather than the specific sequence of the 20 amino-acid helix region is important. When only the 25 amino-acid flexible hinge region was used, the fusion protein tended to aggregate and lose target-binding property (data not shown), similar to that reported in the literature. Figure 1A shows the schematic representation of the gene that codes the FN3$^{\alpha v\beta 3}$-COMP fusion protein. The helical linker region contains a sequence that can be recognized by the biotin protein ligase BirA, an endogenous enzyme that is present in the BL21 strain of *E. coli* used for protein overexpression. By including biotin in the culture medium, the recombinant protein will be enzymatically biotinylated in a site-specific manner during overexpression. Therefore, the resulting affinity molecules can be easily conjugated to other biomolecules or nanomaterials that are linked or coated with streptavidin or neutravidin. To facilitate purification of overexpressed affinity molecules from bacterial cell lysate, a His×6 tag was engineered at the N-terminus followed by a thrombin recognition site.

Expression, Self-Assembly, and Purification of FN3$^{\alpha v\beta 3}$ Pentamer. FN3$^{\alpha v\beta 3}$ is a FN3 based monobody that binds to $\alpha_v\beta_3$ integrin with high affinity and specificity. This monobody was engineered by optimizing residues surrounding the integrin-binding RGD sequence in the flexible FG loop with a novel RGDWXE consensus sequence (*17*). We overexpressed in *E. coli* the monomeric FN3$^{\alpha v\beta 3}$ that does not contain the COMP pentamerization domain and the fusion

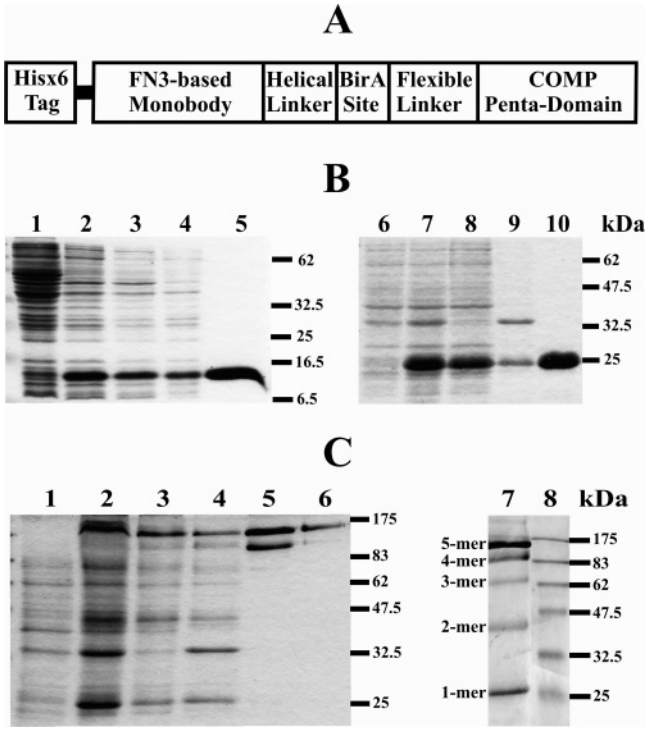

FIGURE 1: (A) Schematic representation of the FN3$^{\alpha v\beta 3}$-COMP fusion protein. The linkage between the His×6 tag and the FN3 monobody domain represents a cleavage site that can be removed by thrombin. (B) SDS-PAGE analysis of the expression and purification of the overexpressed monomeric FN3$^{\alpha v\beta 3}$ (left panel) and pentameric FN3$^{\alpha v\beta 3}$-COMP (right panel) under reducing conditions: lanes 1 and 6, total protein after noninduced expression; lanes 2 and 7, total protein after induced expression; lanes 3 and 8, soluble fraction of induced expression; lanes 4 and 9, insoluble fraction of induced expression; lanes 5 and 10, soluble fraction after first IMAC purification. (C) SDS-PAGE analysis of the expression and purification of the overexpressed pentameric FN3$^{\alpha v\beta 3}$-COMP under nonreducing conditions: lane 1, total protein after noninduced expression; lane 2, total protein after induced expression; lane 3, soluble fraction of induced expression; lane 4, insoluble fraction of induced expression; lane 5, soluble fraction after first IMAC purification; lane 6, soluble fraction after second IMAC purification using gradient elution; lane 7, soluble fraction of induced expression when more proteins were loaded to reveal multimers; lane 8, molecular weight markers.

protein FN3$^{\alpha v\beta 3}$-COMP that can self-assemble into a pentameric form. Figure 1B shows the SDS-PAGE analysis of expression and purification of monomeric and pentameric forms under reducing conditions, whereas Figure 1C shows the analysis of FN3$^{\alpha v\beta 3}$-COMP fusion protein under nonreducing conditions. Both FN3$^{\alpha v\beta 3}$ and FN3$^{\alpha v\beta 3}$-COMP were expressed very well, with a soluble expression level at 40 and 12 mg/L, respectively. FN3$^{\alpha v\beta 3}$ does not contain COMP domain, and therefore is always present as a monomer under both reducing and nonreducing conditions. However, the FN3$^{\alpha v\beta 3}$-COMP fusion protein can self-assemble into multimeric forms with high efficiency. While most of the protein in the supernatant of the lysed cells was present as the pentameric form, the monomer, dimer, trimer, and tetramer could be detected when more proteins were loaded on a nonreducing SDS-PAGE gel (Figure 1C, lane 7). Although we just expressed the FN3$^{\alpha v\beta 3}$-COMP fusion protein in the cytosol of *E. coli*, we postulate that self-assembly could be more efficient if the fusion protein is expressed in the periplasm of *E. coli* where disulfide bonds would directly form at residues 29 and 30.

After purification using an IMAC loaded with Ni^{2+}, the monomeric, dimeric, and trimeric forms were almost undetectable and a vast majority of the purified protein was in its tetrameric and pentameric forms (Figure 1C, lane 5). One possibility is that the immobilization on IMAC increases the local concentration of FN3 monobody and therefore facilitates its self-assembly into tetramer and pentamer. Using an HABA-avidin assay, we found that approximately 35−40% of the fusion protein was biotinylated when the expression was carried out in BL21 *E. coli* strain in the presence of externally added biotin. The level of biotinylation should be higher when an *E. coli* strain with overexpressed BirA is used. We also performed overexpression without the addition of free biotin to the bacterial culture. The proteins thus generated and purified were then chemically biotinylated using NHS−PEO_4−biotin to obtain monobodies with an average of one biotin per monomer or pentamer for different assays.

Separation of the pentamer from the tetramer is challenging. The molecular weights of these two forms differ by only 20 000, which could not be resolved by a gel filtration column such as Superdex G-200. We found that these two forms could be separated using an IMAC column through gradient elution. The pentameric form contains five His×6 tags and is therefore captured more tightly by IMAC than the tetrameric form. This is presumably due to the avidity effect of the binding between the fusion protein and the Ni−NTA moiety on the solid surface, and probably also due to a lower stability of the tetramer. This allows the removal of the tetramer by sequential increase of the concentration of imidazole during elution. Through this procedure, the pentameric form was effectively separated from the tetramer (Figure 1C, lane 6). However, a faint tetramer band was still visible in the purified pentamer fraction. It appears that the majority of the protein is tetramer or pentamer, and both should have high avidity.

FN3$^{\alpha v\beta 3}$ Pentamer Bound to $\alpha_v\beta_3$ with Significantly Improved Strength. With the availability of purified monobodies, we first examined the integrin-binding properties of both monomer and pentamer by ELISA analysis. Figure 2A demonstrates that the monomer and pentamer bound to $\alpha_v\beta_3$ in a concentration dependent manner. It appears that the pentamer bound more tightly to $\alpha_v\beta_3$ when compared to the monomer at all concentrations tested (0.1 nM to 100 nM). Figure 2B shows that the pentameric form bound to $\alpha_v\beta_3$ with a signal much higher than that of the monomer, when both proteins were used at a much lower concentration (25 nM). At such low concentration, the binding of the monomer to $\alpha_v\beta_3$ was difficult to detect by ELISA, although it could be confirmed by more sensitive BIAcore analysis. When other integrins including $\alpha_1\beta_1$, $\alpha_5\beta_1$, and $\alpha_v\beta_5$ were used to coat the plate, the signals were close to background. We further compared the target-binding strength of the monomer and the pentamer using a membrane blotting approach. To this end, different concentrations of the monomer and the pentamer were blotted on a nitrocellulose membrane. The blots were then incubated with $\alpha_v\beta_3$, and the binding was detected using an anti-$\alpha_v\beta_3$ antibody coupled with anti-Ig-HRP. As shown in Figure 2C, the binding of the pentamer to $\alpha_v\beta_3$ was much stronger than that of the monomer, despite that the used concentration of the pentamer was 200 times lower than that of the monomer.

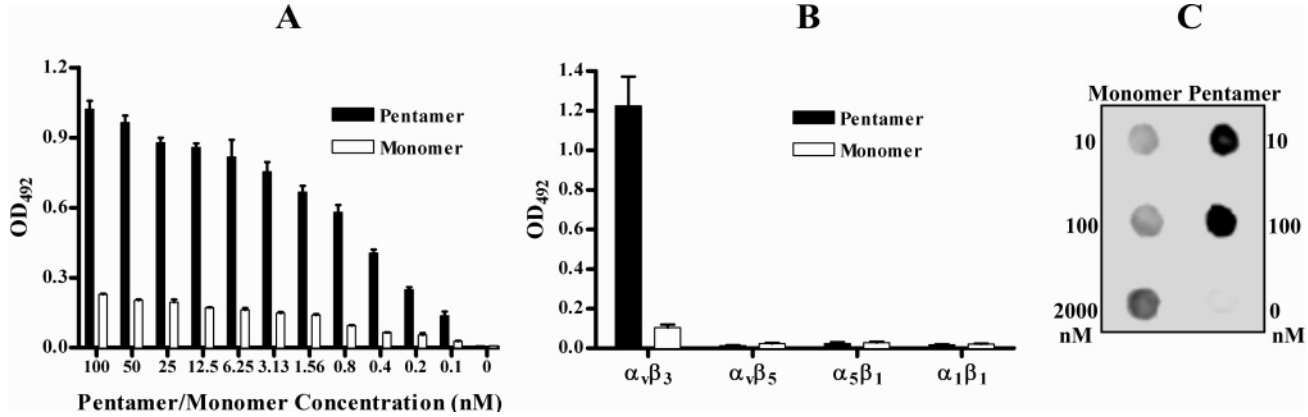

FIGURE 2: Assessment of integrin binding of monomeric and pentameric monobodies by ELISA. (A) Comparison of the binding of monomer and pentamer to $\alpha_v\beta_3$. Purified $\alpha_v\beta_3$ and BSA (as control) were coated in different wells of an EIA/RIA plate. Biotinylated monomer and pentamer were added at different concentrations from 0 to 100 nM. The signal was generated by neutravidin-HRP using OPD as a substrate. (B) Comparison of the binding of monomer and pentamer to different integrins. Purified $\alpha_1\beta_1$, $\alpha_5\beta_1$, $\alpha_v\beta_3$, $\alpha_v\beta_5$, and BSA were coated on the plate. Biotinylated monomer and pentamer were added at 25 nM. The background (binding of biotinylated monobody with coated BSA) was subtracted from all the readings, and the mean of triplicate determinations was used to prepare the diagram. (C) Comparison of the binding of monomer and pentamer to $\alpha_v\beta_3$ using dot blotting. Monomer or pentamer was spotted at various concentrations (10 nM to 2 μM) onto nitrocellulose membranes. The blots were incubated with 5 μg/mL of $\alpha_v\beta_3$ and probed with an anti-$\alpha_v\beta_3$ antibody followed by detection using anti-mouse Ig-HRP as the secondary antibody.

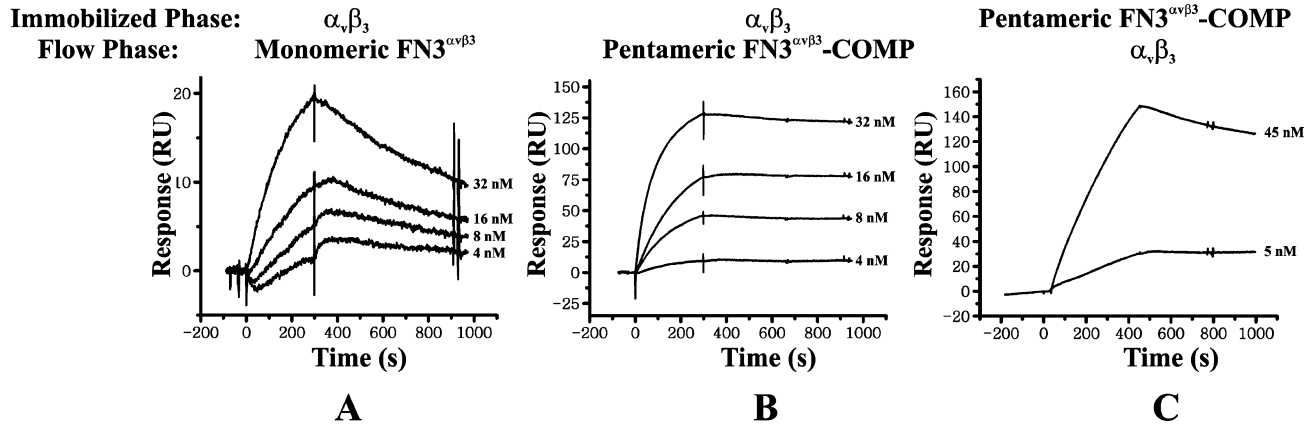

FIGURE 3: BIAcore analysis of target-binding properties of monomeric FN3$^{\alpha v\beta 3}$ and pentameric FN3$^{\alpha v\beta 3}$-COMP to integrins. (A) Binding of monomeric FN3$^{\alpha v\beta 3}$ (4, 8, 16, and 32 nM) to immobilized $\alpha_v\beta_3$. (B) Binding of pentameric FN3$^{\alpha v\beta 3}$-COMP (4, 8, 16, and 32 nM) to immobilized $\alpha_v\beta_3$. (C) Binding of $\alpha_v\beta_3$ (5 and 45 nM) to immobilized pentameric FN3$^{\alpha v\beta 3}$-COMP. Analyses were performed at room temperature in HBS−P buffer supplemented with 2 mM $CaCl_2$ at a flow rate of 20 μL/min. Measurements at higher flow rates were also performed but not shown here.

Table 1: Binding Constants of Monomeric and Pentameric Monobodies to Immobilized $\alpha_v\beta_3$ Using BIAcore Analysis

monobody	K_{on} (L/(mol·s))	K_{off} (s^{-1})	K_D (mol/L)
pentameric FN3$^{\alpha v\beta 3}$-COMP	7.54×10^5	$<10^{-5}$	$<1.3 \times 10^{-11}$
monomeric FN3$^{\alpha v\beta 3}$	1.48×10^5	1.01×10^{-3}	6.82×10^{-9}

The $\alpha_v\beta_3$-binding constants of monomer and pentamer were measured by surface plasmon resonance (SPR) using BIAcore CM5 sensor chips with $\alpha_v\beta_3$ integrin immobilized. To examine the multivalent effect, relatively low concentrations of monobodies were used in the flow phase. As shown in Figure 3A, the monomeric FN3$^{\alpha v\beta 3}$ rapidly dissociated from the surface immobilized $\alpha_v\beta_3$. The binding affinity of monomer thus measured is approximately 6.82 nM (Table 1), close to that estimated in the literature (*17*). Significantly, the pentameric FN3$^{\alpha v\beta 3}$-COMP dissociated from the surface immobilized $\alpha_v\beta_3$ much more slowly compared to the monomer (Figure 3B). The dissociation process of the pentamer was multiphasic and difficult to model, which is a characteristic of multivalent interactions (*21*). To compare the monomer and the pentamer on the same surface, the BIAcore data were fitted to a 1:1 interaction model. The approximation off-rate of the pentamer is less than 10^{-5} s^{-1}. Therefore, the avidity of the pentamer to $\alpha_v\beta_3$ should be less than 13 pM, which is much stronger than the affinity of the monomeric form. To address the possible rebinding issue, we compared the binding of the pentamer to immobilized $\alpha_v\beta_3$ at flow rates from 20 to 60 μL/min. No difference was detected when the flow rate was tripled, suggesting that rebinding was not obvious under the conditions we used (data not shown). However, it should be noted that the measured binding strength strongly depends on the experimental conditions, particularly the receptor density on the surface as reported in the literature (*29*). The estimated half-life of dissociation of the pentameric form from the SPR experiment was very long. Since SPR traces can only be recorded within

hours rather than days, it is difficult to accurately determine such a slow off-rate. Therefore, the SPR measured off-rate is a rough estimation rather than an accurate determination. However, it still provides valuable information for comparison of the binding of the monomer and the pentamer to surface immobilized integrins. We also prepared CM5 chips with neutravidin immobilized. These chips were loaded with biotinylated monobodies followed by a passage of $\alpha_v\beta_3$ with different concentrations. Similar binding constants were obtained when the pentamer was compared with the monomer (Figure 3A, C). This result suggests that pentamerization did not significantly change the accessibility of the interaction sites.

Target-Binding Specificity of Monomer Retained on Pentamer. While pentamerization can significantly increase the target-binding strength, it is of great importance to examine whether its target-binding specificity is still maintained. Most RGD-containing peptides bind to both $\alpha_v\beta_3$ and $\alpha_v\beta_5$. However, the FN3 monobody used here was developed to specifically bind to $\alpha_v\beta_3$, but not to $\alpha_v\beta_5$ (*17*). This allows us to investigate whether the integrin-binding specificity of the monomer was altered after pentamerization. To this end, we prepared CM5 chips with $\alpha_5\beta_1$ or $\alpha_v\beta_5$ immobilized, and passed through the chip either the monomer or the pentamer to test their specificity. The binding of the pentamer to $\alpha_5\beta_1$ or $\alpha_v\beta_5$ integrins was not detectable (data not shown), indicating that the pentamer possesses the same integrin-binding specificity as that of the monomer.

FN3$^{\alpha v\beta 3}$ Pentamer Resistant to Protease Digestion and Heat-Induced Denaturation. A good affinity molecule should have exceptional stability against both protease digestion and thermal-induced denaturation. One of the most important features of FN3 monobody is its exceptional stability. To examine whether such stability was retained in the pentameric form, we first compared its protease resistance with that of the monomer using thermolysin, a thermostable extracellular metalloendopeptidase that is widely used to perform limited proteolysis for peptide mapping and studies of protein structure and conformational changes (*30*). The purified monomer and pentamer were incubated with thermolysin at various temperatures between 4 and 42 °C under both nonreducing and reducing conditions. When digested with protease under nonreducing conditions, the monomer was partially truncated to a fragment that could not be further degraded (Figure 4A-1). Such truncation was efficient when the reaction was carried out at 25 °C. Since a His×6 tag was fused to the N-terminus via a thrombin cleavage site, it is likely that the observed truncation was due to the removal of this flexible affinity tag. Compared to the monomer, the pentameric form exhibited a much better resistance without any obvious degradation to thermolysin digestion throughout the examined temperature range (Figure 4A-3). Interestingly, the suspected removal of the affinity tag was observed only on the monomer but not on the pentamer, when proteolytic reactions were performed under nonreducing conditions (Figure 4A-1, A-3). To reveal the digestion details of the pentamer that could not be resolved on a nonreducing SDS-PAGE gel due to its high molecular weight, the same digestion samples were loaded onto a gel that was run under reducing conditions. Figure 4A-4 shows that only a slight digestion was observed when the proteolysis was performed at 42 °C, indicating the pentamer was indeed protease-resistant throughout the temperature range. These results strongly imply that the pentameric structure is not as accessible to the protease as the monomer, presumably because the pentameric form is well-folded with higher stability than the already very stable monomer. We also compared the protease resistance when the proteolysis was performed under reducing conditions in which the pentamer was also present as a monomeric form. Parts A-2 and A-5 of Figure 4 show that both the monomer and the pentamer were truncated efficiently at 37 °C. It seems that the pentamer

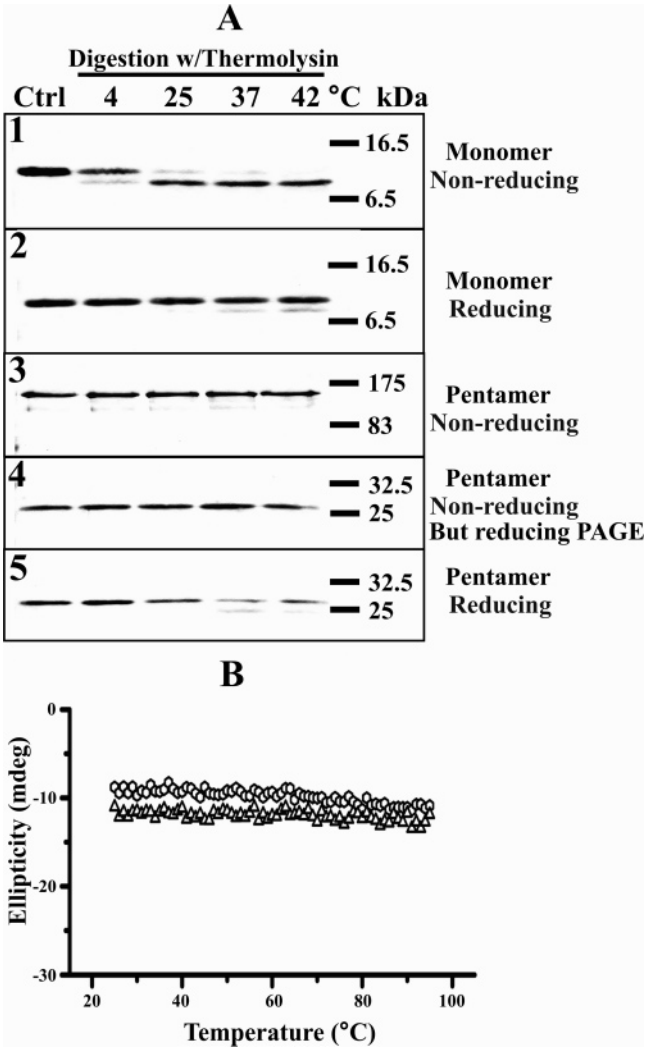

FIGURE 4: (A) Sensitivity of monomeric and pentameric monobodies to thermolysin. The digestion was performed by mixing 2 μg of purified monomeric or pentameric monobody with 20 ng of thermolysin for 15 min at 4, 25, 37, and 42 °C, respectively, under both reducing and nonreducing conditions: (1) digestion of monomeric FN3$^{\alpha v\beta 3}$ under nonreducing conditions, (2) digestion of monomeric FN3$^{\alpha v\beta 3}$ under reducing conditions; (3) digestion of pentameric FN3$^{\alpha v\beta 3}$-COMP under nonreducing conditions; (4) digestion of pentameric FN3$^{\alpha v\beta 3}$-COMP under nonreducing conditions, but the SDS-PAGE gel was run under reducing conditions; (5) digestion of FN3$^{\alpha v\beta 3}$-COMP under reducing conditions. (B) Heat-induced denaturation curves for monomeric FN3$^{\alpha v\beta 3}$ and pentameric FN3$^{\alpha v\beta 3}$-COMP. The analyses were performed in 10 mM phosphate buffer at pH 7.5. Sample temperatures were increased gradually from 25 to 95 °C. Spectra were recorded at various temperatures following a 10 min equilibration time. An average of multiple measurements of the ellipticities at 215 nm with 70 μg/mL of monomeric FN3$^{\alpha v\beta 3}$ or that at 209 nm with 40 μg/mL of pentameric FN3$^{\alpha v\beta 3}$-COMP was used to plot the graph of ellipticity versus temperature.

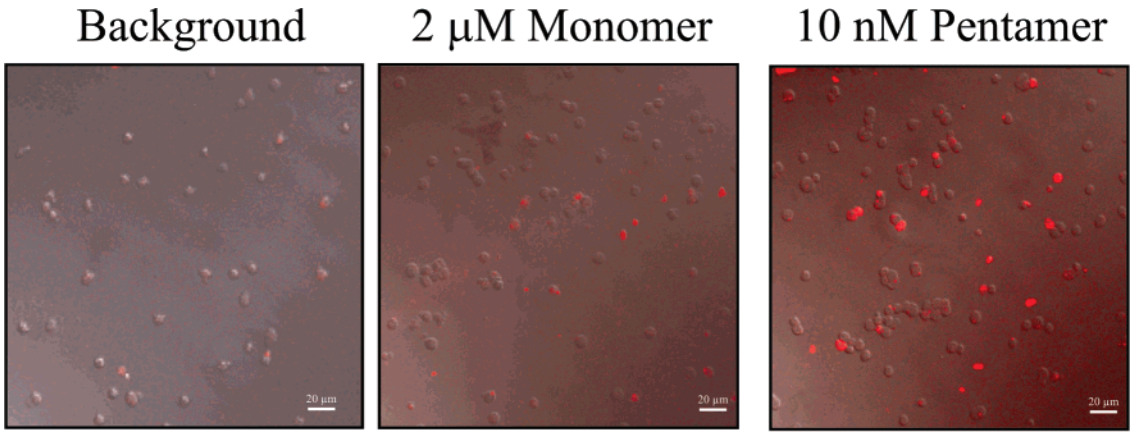

FIGURE 5: Comparison of the binding of monomer and pentamer to K562-$\alpha_v\beta_3$ cells using confocal microscopy. Biotinylated monomer (2 μM) or pentamer (10 nM) were mixed with streptavidin−Alexa Fluor 555 and incubated with K562-$\alpha_v\beta_3$ cells. Monobody was not included in the control. After binding and washing, cells were mounted onto slides and examined using a confocal microscope.

was digested to a larger extent, presumably due to the presence of a flexible linker region between the FN3 and the COMP domains. Since the pentameric monobody thus generated is used to target extracellular rather than intracellular biomarkers, such instability under reducing conditions should not be a concern.

To determine the thermal stability of these monobodies, circular dichroism (CD) spectra of both the monomer and the pentamer were measured at various temperatures (Figure 4B). Consistent with previous reports, the monomer was very stable during the entire temperature range (25−95 °C) we tested, although there was a slight decrease of ellipticity when the temperature exceeded 80 °C. It seems that the pentamer is also stable. No obvious change in the CD spectra of the pentamer was observed, even when the temperature was over 90 °C. The T_m values could not be determined in both cases. These results suggest that the pentameric monobody is at least as stable as the monomeric form. However, it is also possible that the spectra of the protein might not change in response to increasing temperatures if it is unfolded.

FN3$^{\alpha v\beta 3}$ Pentamer Bound to $\alpha v\beta 3$ with Significantly Improved Strength in Integrin-Expressing Cell Lines. Because the avidity effect is highly dependent on the target density on the surface, it is of great interest to examine whether the pentamer is indeed more effective in interacting with the target receptor on the cell surface. To this end, three different cell lines were used, including wild-type K562 ($\alpha_5\beta_1$-positive), K562-$\alpha_v\beta_3$, and K562-$\alpha_v\beta_5$. The latter two cell lines had been stably transfected with $\alpha_v\beta_3$ and $\alpha_v\beta_5$ integrins, respectively. These cells were incubated with an appropriate amount of biotinylated monomeric or pentameric monobodies, prior to the confocal detection of cell surface-bound proteins using streptavidin−Alexa Fluor 555. It was found that both the monomer and the pentamer bound to K562-$\alpha_v\beta_3$ cells, but not to wild-type K562 or K562-$\alpha_v\beta_5$ cells (data not shown). The results from the confocal experiments demonstrate that the pentamer is much more effective than the monomer. As shown in Figure 5, 10 nM of the pentamer was better than 2000 nM of the monomer in specifically staining K562-$\alpha_v\beta_3$ cells. Therefore, the FN3$^{\alpha v\beta 3}$ pentamer bound to $\alpha_v\beta_3$ expressed on the cell surface with at least 200-fold increase in target-binding strength. Since the confocal method is less sensitive than the SPR approach, it is likely that the real increase in targeting binding is more than 200-fold. Interestingly, about 20% of the stained areas by the pentamer had no cells, possibly due to the dislodgement of extracellular matrix during cell washes prior to confocal microscopy detection. Five independent miscroscopy experiments revealed similar results.

DISCUSSION

Unlike display of short peptides with just a few amino acids, display of five protein domains each with a size bigger than the COMP pentameric core itself without losing the right geometry is challenging. The COMP domain based pentameric core is very compact and rigid, with a diameter of just about 20 Å. It is believed that such rod-shaped pentameric structure is not suitable for displaying large peptides or protein domains that require greater interunit spacing (*23*). Indeed, protein domains displayed on COMP scaffold were usually produced as insoluble inclusion bodies in *E. coli* and should undergo refolding to acquire desired functionality (*31*). As reported in the literature, only about a 10-fold increase in binding strength was observed for COMP displayed pentameric protein domains, compared to more than a 10^5-fold increase in pentameric short peptides (*22*, *32*).

We found that the target-binding strength of the pentameric FN3$^{\alpha v\beta 3}$-COMP was significantly increased compared to that of the monomeric form. The success of displaying the pentameric FN3 monobody on a COMP domain does not necessarily mean that other non-FN3 domains can be displayed with the same efficiency. The fusion of several small proteins with a COMP domain had been investigated (*31*, *33*, *34*). However, these fusion proteins were usually produced as insoluble inclusion bodies when overexpressed in bacteria, presumably due to the presence of cysteine residues that could disrupt the formation of a stable pentameric core. Indeed, the target-binding strength of the pentameric Fas domain displayed on a COMP scaffold was increased just 9-fold compared with that of the Fas-Fc, whereas there was no increase for the pentameric TRAIL-R2 (*33*). Recently, the pentameric EGF displayed on COMP was found to have a stronger antiproliferative effect on cancer cell lines overexpressing EGF the receptor. In general, the modest increase in the target-binding strengths of these pentameric protein domains was drastically different from that of pentameric peptides, which often have a 10^5-fold

increase compared with their monomeric forms. On the basis of our results, we hypothesized that the FN3 domain has several unique features that make it an ideal scaffold for pentamerization by using a COMP domain. First, FN3 based proteins can be engineered to be highly expressed in *E. coli* as soluble proteins without the necessity of refolding, as we demonstrated here for both the monomeric and the pentameric $\alpha_v\beta_3$-binding monobodies. Even if the FN3 monobody of interest is present in the inclusion body, its refolding should be more efficient since FN3 domains usually do not contain cysteine residues. The significant increase of the target-binding strength of the pentameric form without changing its target specificity indicates that the pentameric geometry of the fusion protein could be well maintained. We attributed this to the use of an extended linker that provides greater interunit spacing so that five FN3 monobodies can be properly folded without disrupting the pentameric structure. Since multiple affinity units are present to the target of interest at a very close distance, the free energy of target binding with the pentamer should be much greater than that with the monomer.

The unique features of FN3 based pentameric monobody make it a valuable complement to the conventional antibody fragments, particularly as high-avidity biochemical reagents for in vitro applications such as blotting and cell staining. Such monobody might also have the potential to be used under in vivo conditions. FN3 is very abundant in humans. Although the COMP domain used in this work has a mouse origin, a human COMP domain is highly homologous and therefore should work as well. Therefore, the resulting fusion protein might be less immunogenic. However, immunogenicity could still be raised from other sequences such as the linker and the affinity tags. Therefore, further work should be performed to improve the fusion protein. It is believed that FN3 monobodies will be rapidly cleared by the kidneys due to their low molecular weights. The molecular weight of a pentameric FN3 is close to 100 000, compared to just 12 000 of the monomer. Therefore, the clearance of the pentameric FN3 monobodies by the kidneys could be slowed down.

Although the pentameric monobody we demonstrated here is for binding with $\alpha_v\beta_3$, the approach should be applied to other FN3 monobodies for rapid generation of affinity molecules with significantly improved target-binding strengths. Indeed, we found that the VEGF receptor-binding FN3 monobody could be similarly pentamerized to acquire desired avidity (data not shown). Finally, it is worth mentioning that pentamerization of FN3 monobodies should not be limited by using a COMP domain. A novel pentamerization domain such as the nontoxic verotoxin B-subunit developed by MacKenzie and co-workers might also be exploited (*23*).

ACKNOWLEDGMENT

We thank Drs. Ashutosh Tripathy, Biao Dong and Baocheng Huang and Mr. Steve Cotten for assistance in experimental techniques.

REFERENCES

1. Main, A. L., Harvey, T. S., Baron, M., Boyd, J., and Campbell, I. D. (1992) The three-dimensional structure of the tenth type III module of fibronectin: An insight into RGD-mediated interactions, *Cell 71*, 671−678.
2. Carr, P. A., Erickson, H. P., and Palmer, A. G., 3rd. (1997) Backbone dynamics of homologous fibronectin type III cell adhesion domains from fibronectin and tenascin, *Structure 5*, 949−959.
3. Leahy, D. J., Hendrickson, W. A., Aukhil, I., and Erickson, H. P. (1992) Structure of a fibronectin type III domain from tenascin phased by MAD analysis of the selenomethionyl protein, *Science 258*, 987−991.
4. Leahy, D. J., Aukhil, I., and Erickson, H. P. (1996) 2.0 Å crystal structure of a four-domain segment of human fibronectin encompassing the RGD loop and synergy region, *Cell 84*, 155−164.
5. Dickinson, C. D., Veerapandian, B., Dai, X. P., Hamlin, R. C., Xuong, N. H., Ruoslahti, E., and Ely, K. R. (1994) Crystal structure of the tenth type III cell adhesion module of human fibronectin, *J. Mol. Biol. 236*, 1079−1092.
6. Bork, P., and Doolittle, R. F. (1992) Proposed acquisition of an animal protein domain by bacteria, *Proc. Natl. Acad. Sci. U.S.A. 89*, 8990−8994.
7. Jones, E. Y. (1993) The immunoglobulin superfamily, *Curr. Opin. Struct. Biol. 3*, 846−852.
8. Bork, P., Holm, L., and Sander, C. (1994) The immunoglobulin fold. Structural classification, sequence patterns and common core, *J. Mol. Biol. 242*, 309−320.
9. Campbell, I. D., and Spitzfaden, C. (1994) Building proteins with fibronectin type III modules, *Structure 2*, 333−337.
10. Harpaz, Y., and Chothia, C. (1994) Many of the immunoglobulin superfamily domains in cell adhesion molecules and surface receptors belong to a new structural set which is close to that containing variable domains, *J. Mol. Biol. 238*, 528−539.
11. Koide, A., Bailey, C. W., Huang, X., and Koide, S. (1998) The fibronectin type III domain as a scaffold for novel binding proteins, *J. Mol. Biol. 284*, 1141−1151.
12. Koide, A., Jordan, M. R., Horner, S. R., Batori, V., and Koide, S. (2001) Stabilization of a fibronectin type III domain by the removal of unfavorable electrostatic interactions on the protein surface, *Biochemistry 40*, 10326−10333.
13. Batori, V., Koide, A., and Koide, S. (2002) Exploring the potential of the monobody scaffold: Effects of loop elongation on the stability of a fibronectin type III domain, *Protein Eng. 15*, 1015−1020.
14. Karatan, E., Merguerian, M., Han, Z., Scholle, M. D., Koide, S., and Kay, B. K. (2004) Molecular recognition properties of FN3 monobodies that bind the Src SH3 domain, *Chem. Biol. 11*, 835−844.
15. Kwon, Y., Han, Z., Karatan, E., Mrksich, M., and Kay, B. K. (2004) Antibody arrays prepared by cutinase-mediated immobilization on self-assembled monolayers, *Anal. Chem. 76*, 5713−5720.
16. Xu, L., Aha, P., Gu, K., Kuimelis, R. G., Kurz, M., Lam, T., Lim, A. C., Liu, H., Lohse, P. A., Sun, L., Weng, S., Wagner, R. W., and Lipovsek, D. (2002) Directed evolution of high-affinity antibody mimics using mRNA display, *Chem. Biol. 9*, 933−942.
17. Richards, J., Miller, M., Abend, J., Koide, A., Koide, S., and Dewhurst, S. (2003) Engineered fibronectin type III domain with a RGDWXE sequence binds with enhanced affinity and specificity to human alphavbeta3 integrin, *J. Mol. Biol. 326*, 1475−1488.
18. Parker, M. H., Chen, Y., Danehy, F., Dufu, K., Ekstrom, J., Getmanova, E., Gokemeijer, J., Xu, L., and Lipovsek, D. (2005) Antibody mimics based on human fibronectin type three domain engineered for thermostability and high-affinity binding to vascular endothelial growth factor receptor two, *Protein Eng., Des. Sel. 18*, 435−444. Epub Aug. 8, 2005.
19. Dutta, S., Batori, V., Koide, A., and Koide, S. (2005) High-affinity fragment complementation of a fibronectin type III domain and its application to stability enhancement, *Protein Sci. 14*, 2838−2848. Epub Sep 30, 2005.
20. Koide, A., Gilbreth, R. N., Esaki, K., Tereshko, V., and Koide, S. (2007) High-affinity single-domain binding proteins with a binary-code interface, *Proc. Natl. Acad. Sci. U.S.A. 104*, 6632−6637.
21. Pluckthun, A., and Pack, P. (1997) New protein engineering approaches to multivalent and bispecific antibody fragments, *Immunotechnology 3*, 83−105.
22. Terskikh, A. V., Le Doussal, J. M., Crameri, R., Fisch, I., Mach, J. P., and Kajava, A. V. (1997) "Peptabody": A new type of high avidity binding protein, *Proc. Natl. Acad. Sci. U.S.A. 94*, 1663−1668.
23. Zhang, J., Tanha, J., Hirama, T., Khieu, N. H., To, R., Tong-Sevinc, H., Stone, E., Brisson, J. R., and MacKenzie, C. R. (2004) Pentamerization of single-domain antibodies from phage librar-

ies: A novel strategy for the rapid generation of high-avidity antibody reagents, *J. Mol. Biol. 335*, 49−56.
24. Brooks, P. C., Clark, R. A., and Cheresh, D. A. (1994) Requirement of vascular integrin alpha v beta 3 for angiogenesis, *Science 264*, 569−571.
25. Hynes, R. O. (2002) A reevaluation of integrins as regulators of angiogenesis, *Nat. Med. 8*, 918−921.
26. Efimov, V. P., Lustig, A., and Engel, J. (1994) The thrombospondin-like chains of cartilage oligomeric matrix protein are assembled by a five-stranded alpha-helical bundle between residues 20 and 83, *FEBS Lett. 341*, 54−58.
27. Malashkevich, V. N., Kammerer, R. A., Efimov, V. P., Schulthess, T., and Engel, J. (1996) The crystal structure of a five-stranded coiled coil in COMP: A prototype ion channel?, *Science 274*, 761−765.
28. Guo, Y., Kammerer, R. A., and Engel, J. (2000) The unusually stable coiled-coil domain of COMP exhibits cold and heat denaturation in 4−6 M guanidinium chloride, *Biophys. Chem. 85*, 179−186.
29. Pack, P., Muller, K., Zahn, R., and Pluckthun, A. (1995) Tetravalent miniantibodies with high avidity assembling in Escherichia coli, *J. Mol. Biol. 246*, 28−34.
30. Heinrikson, R. L. (1977) Applications of thermolysin in protein structural analysis, *Methods Enzymol. 47*, 175−189.
31. Fattah, O. M., Cloutier, S. M., Kundig, C., Felber, L. M., Gygi, C. M., Jichlinski, P., Leisinger, H. J., Gauthier, E. R., Mach, J. P., and Deperthes, D. (2006) Peptabody-EGF: A novel apoptosis inducer targeting ErbB1 receptor overexpressing cancer cells, *Int. J. Cancer 119*, 2455−2463.
32. Houimel, M., Schneider, P., Terskikh, A., and Mach, J. P. (2001) Selection of peptides and synthesis of pentameric peptabody molecules reacting specifically with ErbB-2 receptor, *Int. J. Cancer 92*, 748−755.
33. Holler, N., Kataoka, T., Bodmer, J. L., Romero, P., Romero, J., Deperthes, D., Engel, J., Tschopp, J., and Schneider, P. (2000) Development of improved soluble inhibitors of FasL and CD40L based on oligomerized receptors, *J. Immunol. Methods 237*, 159−173.
34. Tomschy, A., Fauser, C., Landwehr, R., and Engel, J. (1996) Homophilic adhesion of E-cadherin occurs by a co-operative two-step interaction of N-terminal domains, *EMBO J. 15*, 3507−3514.

BI701215E